ELSEVIER

Materials Science and Engineering B30 (1995) 175–186

MATERIALS SCIENCE & ENGINEERING B

Atomic structure of surfactant monolayers and its role in epitaxial growth

Efthimios Kaxiras

Department of Physics and Division of Applied Sciences, Harvard University, Cambridge, MA 02138, USA

Abstract

The energetically preferred structures of group V adsorbate monolayers on Si and SiGe substrates were studied using first-principles total energy calculations. By comparing structural features of the optimal adsorbate geometries we infer that structures involving self-bonded adsorbate units, such as dimers, trimers or chains, are most likely to segregate easily during growth. Among the group V elements considered, Sb forms structures involving self-bonded adsorbate units on the substrates considered, making it the most promising candidate for a surfactant. This prediction is consistent with recent experiments on Si(111) homoepitaxy. We also consider a simple solid-on-solid model that captures the essential features of surfactant behavior on Si substrates. The model involves a single variable ε_a, the activation energy for exchange between a newly deposited atom and a surfactant unit on a terrace. We find that depending on the temperature, the model leads to smooth or rough overlayers. The transition takes place at $k_B T \approx 0.1\varepsilon_a$. The qualitative difference in growth mode is demonstrated by examining the topological features of films grown under different conditions.

Keywords: Growth; Epitaxy; Semiconductors; Surfactants

1. Introduction

There is at present a concerted effort to produce semiconductor devices with desirable electronic and optical properties beyond the range offered by typical materials such as bulk silicon, germanium, gallium arsenide, etc. This effort has focused on producing artificial structures, including thin films, quantum wells, wires, and dots, often by methods that allow control of the "building" process of the structure at the atomic level (for a review and extended references see Ref. [1]). A number of problems arise in such attempts: lattice mismatch between the substrate and the overlayers leads to creation of defects; interdiffusion at the boundary reduces or eliminates the order at the interface; polarity effects introduce carriers or long-range imperfections (such as antiphase boundaries). These problems can reduce the effectiveness of the artificially grown structures to the point of making them useless for applications. A typical situation arises in lattice-mismatched heteroepitaxial layers, where a high dislocation density is necessary to relieve the strain but can introduce an unacceptable number of electron traps (see for example Ref. [2]).

It is, nevertheless, possible to control growth at the atomic level in certain systems with the proper choice of components and processing methods. A striking illustration of atomic manipulation of growth is the use of monolayers of adsorbates to control the growth mode in the Si–Ge system. (In the present work we use the word "adsorbates" to refer to the foreign atoms that are specifically introduced in a system in order to alter the growth mode. These atoms must be distinguished from the atoms that will form the desired film on the substrate; the latter type of atoms are referred to as "newly deposited" atoms or "overlayers".) In the original work that demonstrated the feasibility of such processes, a monolayer of As was used successfully to control the growth of Ge overlayers on Si(100) substrates [3]. Owing to the lattice mismatch and the balance of surface and interface energies, when Ge is deposited onto bare Si(100) it grows epitaxially for three monolayers but then reverts to island growth. A monolayer of As passivates the Si(100) surface and keeps floating on top of the Ge during growth, allowing the pseudomorphic growth of considerably thicker Ge films, up to at least 15 monolayers. A similar effect was later observed on the Si(111) surface, using a mono-

0921-5107/95/$9.50 © 1995 – Elsevier Science S.A. All rights reserved
SSDI 0921-5107(94)09012-2

layer of Sb. On this substrate, Ge also begins to form islands after three layers, while the addition of a monolayer of Sb leads to pseudomorphic growth of Ge for 30–70 monolayers [4]. More recently, group III atoms were also used as surfactants during growth of Ge on Si(111) [5].

The mode of growth that is observed with or without the adsorbate layers is due to a balance of local thermodynamic equilibrium and kinetic effects. The adsorbate layers have been called "surfactants" [3–5], a term commonly used to describe agents that lower the surface energy. While the group V adsorbate monolayers certainly produce large changes in the surface energy of the Si substrates, they also introduce changes in the kinetics of growth [6] which include diffusion barriers, activation energies for atomic exchanges, etc. For simplicity, we adopt the term surfactant in the present work with the understanding that it applies to a wider range of phenomena than just lowering of surface energy. Thus, the use of this term to describe the effect of a monolayer of As on Si(100), or of Sb on Si(111), does not imply here that the ensuing change in the mode of growth is determined by equilibrium energies alone.

The purpose of the present paper is twofold. First, we examine what are the important structural features that allow some elements to play the role of a surfactant on semiconductor substrates. In order to do this, we consider the structure of monolayers of different group V elements on the Si(111) and Si(100) substrates (including Ge layers), and compare their relative stability using first-principles total energy calculations. Second, we provide a model that addresses the role of a surfactant on the kinetics of growth and explore some of the consequences of this model. This second issue is much too complicated for first-principles calculations. It is treated at a heuristic level, using a solid-on-solid model and Monte Carlo (MC) simulations. Both the detailed first-principles calculations on specific systems and the stochastic simulations of heuristic models are useful for understanding surfactant mediated growth at the atomistic level.

2. Energetics of group V monolayers on Si(100)

The original experimental work on the Si–Ge system showed that As was a good choice of surfactant [3]. Other group V elements, such as Sb, behave in the same manner on the Si(100) substrate. The structure of group V layers on Si(100) is similar to the structure of the bare substrate, with the adsorbate atoms forming dimer rows, as shown in Fig. 1. All group V elements form the same reconstruction on this substrate. The structure with the group V layer on the surface is much more stable than the bare substrate. The group V dimers render each group V atom chemically passive, with three of its five valence electrons participating in the formation of covalent bonds, two bonds with substrate Si atoms and one bond with another group V atom. The remaining two valence electrons of the group V elements are in a low energy lone-pair orbital. Once the group V dimers have formed on the surface, all the Si atoms become four-fold coordinated, in an essentially ideal geometry (except for small relaxation to accommodate the adsorbate dimers, see Fig. 1). In contrast, the bare substrate involves dangling bond orbitals on the surface Si atoms which remain three-fold coordinated, giving rise to a less passive structure.

When Ge layers are deposited onto the As or Sb covered Si(100) substrate, the group V dimers segregate to the top layer. The mechanism by which this segregation is made possible is not known, although interesting models have been proposed to explain it [7–9]. It is, however, evident that there exists an energetic incentive for the segregation. The energy of configurations with the group V dimers on top is much lower than the energy of structures where the group V layers are embedded below layers of Ge or Si. This fact has been established through first-principles calculations of the relative energies (for details on the computational methodology see Apprendix A). Since all group V adsorbates form the same structure on this surface, we concentrate on the case of As. The other two group V candidates (P and Sb) exhibit the same qualitative behavior. The relevant energy comparisons are given in Table 1. In all the structures studied the surface layer consists of a (2×1) dimer reconstruction. For comparison, we also give the relative energy of a Ge layer being on top of the Si(100) surface vs. being embedded below a Si layer. The energetically preferred configuration consists of the Ge layer on the surface.

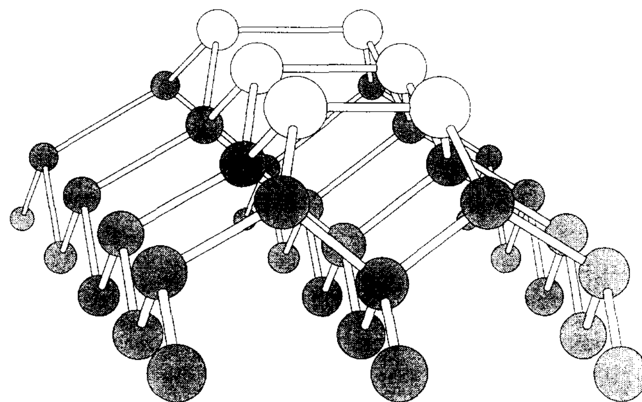

Fig. 1. The structure of As-covered Si(1000). All the substrate atoms (shaded spheres) are four-fold coordinated, while As dimer rows (open spheres) are formed on the surface.

This is expected, since the surface energy of Ge is lower than that of Si. The tendency of group V layers to be on the surface is much stronger than for the Ge layer. The energy difference between structures that have the group V layer on the surface or embedded below the surface is more than an order of magnitude larger than the corresponding energy difference for the Ge layer (see Table 1). Thus, assuming that the segregation is not kinetically inhibited, there exists a strong energy incentive for the group V layers to keep floating on top of any Ge deposited during growth.

The energetically driven segregation of the surfactants is a necessary but not sufficient condition for manipulation of the growth mode. The necessity of having segregation of the adsorbates during growth is obvious, since in the absence of segregation the buried adsorbates would very quickly (after a couple of layers of deposition) cease to affect growth. However, the segregation alone does not lead automatically to enhancement of pseudomorphic layered growth; it must also affect the kinetics of growth [6], making the formation of three-dimensional islands of Ge unfavorable. A macroscopic treatment of the dynamical effects in surfactant-mediated growth has been recently discussed in terms of continuum equations [10]. A possible microscopic model that can lead to layered growth in the presence of surfactants is proposed and analyzed in detail below.

3. Energetics of group V monolayers on Si(111)

In contrast to the Si(100) surface, where the only possible structure is the dimer geometry, a number of atomic arrangements for group V atoms are allowed on the Si(111) surface. All these arrangements must satisfy the bonding requirements of the group V atoms and the substrate atoms, as described in detail in the previous section. This ensures that the surface is properly passivated, so that the surface energy is low. The allowed geometries that fulfill the bonding requirements are shown in Fig. 2. They include two geometries in which the adsorbates form trimer units, with the trimer centre directly above a hexagon composed of first and second layer substrate atoms (Fig. 2(a), referred to as the H_3-trimer), or directly above a second layer substrate atom (Fig. 2(b), referred to as the T_4-trimer). Both trimer reconstructions lead to a $(\sqrt{3} \times \sqrt{3})$ pattern. A third possibility is a chain geometry, Fig. 2(c), which gives rise to a (2×1) periodic pattern. Finally, the last possibility involves a substitutional geometry, Fig. 2(d), in which the adsorbate atoms take the place of the surface Si atoms and give rise to a (1×1) periodic pattern.

Table 1
Comparison of relative energies of different layer sequences on the Si(100) substrate (which is denoted by [...Si...])

Layer sequence	Relative energy
Ge–Si–[...Si...] vs. Si–Ge–[...Si...]	−0.13
As–Ge–[...Si...] vs. Ge–As–[...Si...]	−1.43
As–Si–[...Si...] vs. Si–As–[...Si...]	−2.27

All configurations involve (2×1) dimer reconstructions on the surface. In each case the energy of the first configurations is given with respect to the second. The relative energies are in electron volts per dimer.

There is a qualitative difference in the bonding arrangements of these four geometries. The first three structures involve group-V–group-V bonds, as well as group-V–Si bonds, while the last involves only group-V–Si bonds on the surface. In this respect the substitutional geometry is rather different from all the other geometries, including the dimer structure on the Si(100) substrate, which also involves both group-V–Si as well as group-V–group-V bonds in the adsorbate dimers (see Fig. 1). We refer to units that involve bonds between adsorbate atoms as "self-bonded adsorbate units". We argue that these differences in bonding topology play an important role in the ability of the different elements to segregate to the surface during growth.

Since a variety of structures satisfying the bonding requirements are allowed on the Si(111) substrate, it is important to establish which structure is energetically preferred. This issue is addressed by first-principles quantum mechanical calculations of the total energy of the different geometries (for more details see Ref. [11]). The results for the four different geometries and three different elements (P, As and Sb) are shown in Fig. 3. In each case the lowest energy geometry (substitutional for P and As, T_4-trimer for Sb) is consistent with experimental observations [12–14]. There is a striking difference in the behavior of the three different adsorbates considered. P and As prefer by a large margin to be in the substitutional geometry, whereas Sb prefers either the T_4-trimer or the chain geometry (the energy difference between these two is very small).

These results can be rationalized as a balance between the strength of the various covalent bonds and the strain introduced by bond-length and bond-angle requirements. In Table 2 we give the adsorbate bond strain defined to be the difference between the calculated bond length values and the ideal covalent bond distance (the sum of covalent radii as given by Pauling [15]). For each adsorbate we compare the bond strain in the substitutional geometry and the T_4-trimer geometry, which is representative of the structures involving self-bonded adsorbate units. In the substitutional geometry all three bonds of the adsorbate atoms

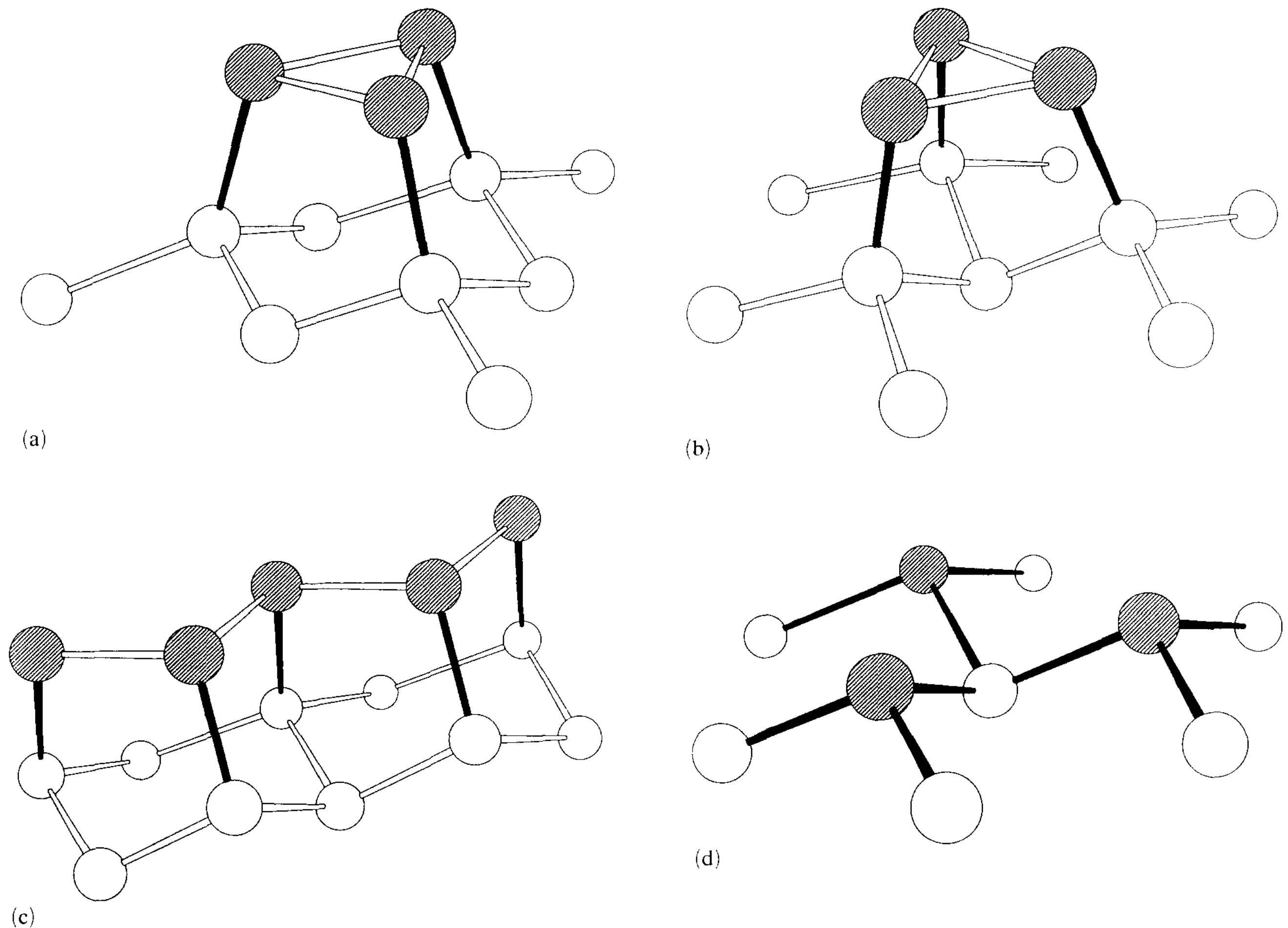

Fig. 2. Geometries for the group V adsorbate layers: (a) H_3-trimer, (b) T_4-trimer, (c) chain, and (d) substitutional. The adsorbate atoms are shown shaded, while the substrate atoms are shown as open spheres. The unlike-atom (adsorbate–substrate) bonds are colored black, to distinguish them from like-atom (adsorbate–adsorbate or substrate–substrate) bonds.

are equivalent. In the trimer geometry (as well as in the other geometries involving self-bonded adsorbate units) each adsorbate atom has one bond to a substrate atom and two bonds to other adsorbate atoms. For the bond strain of the latter geometry we take a weighted average over the different types of bond of the adsorbate atoms. The different types of bond have bond strain of the same sign for all the elements in the two structures compared, so that the numbers given in Table 2 do not represent accidental cancellation of strain. The bond strain analysis reveals that the P structures are in general under tensile stress whereas the As and Sb structures are under compressive stress. This is expected, since P has a smaller covalent radius than Si, whereas for As and Sb the opposite is true. For As and Sb, the structures with the lowest strain (substitutional for As, T_4-trimer for Sb) also have the lowest energy (compare with Fig. 3). This does not hold for the P structures, in which case the lowest energy geometry (substitutional) has higher strain. The reason for this somewhat counter-intuitive finding is the strength of the P–Si bond, which exceeds that of As–Si and Sb–Si bonds, since P and Si are in the same row of the Periodic Table (see, for example bond strength trends in Pauling [15]). Consequently, in the case of P the energetically preferred geometry is that which maximizes the number of P–Si bonds (i.e. the substitutional geometry which has three such bonds per adsorbate atom), despite the small increase in bond strain over geometries that involve fewer P–Si bonds (such as the T_4-trimer, which has one such bond per adsorbate atom).

An interesting question is how are the relative energies of the various geometries affected when Ge is introduced in the system. We investigate this issue for the case of Sb layers. In addition to the structures described so far, we have considered structures in which the Sb layer lies on top of a Ge bilayer deposited

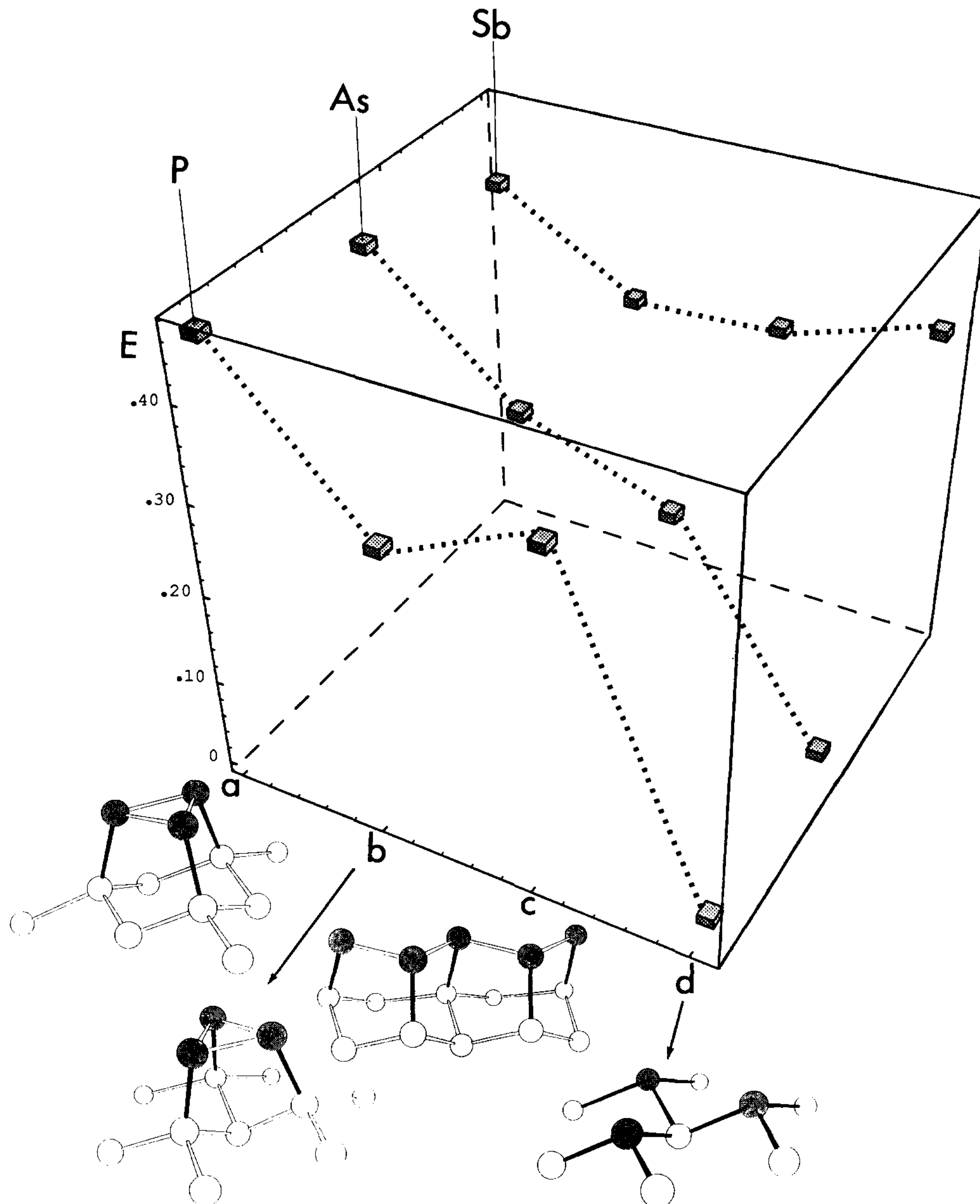

Fig. 3. Relative energies (in electronvolts per adsorbate atom) for the different geometries of the elements P, As and Sb, forming adsorbate layers on the Si(111) substrate. Structures of the same adsorbates are joined by dotted lines. The energies of the T_4-trimer geometries are aligned. The geometries are shown on the horizontal axes with the same labels as in Fig. 2.

onto the Si substrate, as well as structures in which the adsorbate layer is on top of a Ge substrate. The latter represents the case where a large amount of Ge has been deposited onto the Si substrate so that the Ge layers are relaxed to their bulk lattice constant. In the first case, i.e. when a Ge bilayer has been deposited onto the Si substrate, the lowest energy adsorbate geometry becomes the chain structure, with the T_4-trimer structure having slightly higher energy. This ordering is the reverse of that found for Sb layers on the Si(111) substrate (see Fig. 3), but in both cases the energy difference between these two lowest energy geometries is rather small. In the second case, where the Sb layer is on top of a Ge substrate, the lowest energy geometry is the substitutional geometry. This is not surprising, since the lattice constant of Ge is about 4% larger than that of Si. This size difference eliminates the bond strain in the substitutional geometry for Sb on Si(111) (see Table 2) and makes it energetically preferred.

These comparisons suggest the following scenario. When Sb is deposited onto Si(111) it assumes the T_4-

Table 2
Adsorbate bond strain in two different geometries on the Si(111) substrate

Adsorbate	Substitutional (%)	T_4-trimer (%)
P	+4.2	+1.5
As	−0.9	−2.7
Sb	−3.5	−1.9

In the substitutional geometry (Fig. 1(d)) all adsorbate-substrate bonds are equivalent. In the T_4-trimer geometry (Fig. 1(b)) each absorbate has two bonds to other adsorbate atoms and one bond to the substrate. The bond strain is defined as the deviation of the calculated value from the ideal covalent bond distance as given by Pauling [15]. For the T_4-trimer geometry a weighted average over the different types of bonds is taken.

trimer geometry in a pattern with $(\sqrt{3} \times \sqrt{3})$ periodicity. On deposition of a Ge bilayer, the Sb structure changes to the chain geometry with a (2×1) periodicity. This is consistent with experimental observations [4,14]. The chain structure should persist for a while during growth. When a large amount of Ge has been deposited, eventually the equilibrium structure should be the substitutional geometry. This sequence of structural transitions brings up the question of kinetic effects: is it possible to pass from one structure to another without being hindered by large energy barriers? Questions of this type are generally much more difficult to address, because the pathways for structural transformations are not known. However, one can make plausibility arguments about the likelihood of kinetic barriers, based on the structural features of the different geometries. In particular, both the trimer and the chain geometries have the same connectivity. Specifically, in both of these structures each group V atom has two other group V atoms as neighbors and is bonded to one substrate Si atom. In going from one structure to the other, the basic connectivity of each atom need not be changed.

A particular pathway that achieves this structural change with an interchange of a single covalent bond per triplet of group V atoms is illustrated in Fig. 4. Here the trimer structure (in this case consisting of a T_4-trimer and an H_3-trimer at adjacent positions) is changed into a chain structure by forming bonds between atoms connected by dashed lines in Fig. 4(a) and by eliminating bonds between atoms connected by dotted lines in Fig. 4(b). This type of bond switching is known to be a relatively low activation energy process on semiconductor surfaces, as in the formation of the (2×1) π-bonded chain reconstruction on Si(111) by cleavage [16–18]. Moreover, few such bond switches need to take place in order to achieve the structural

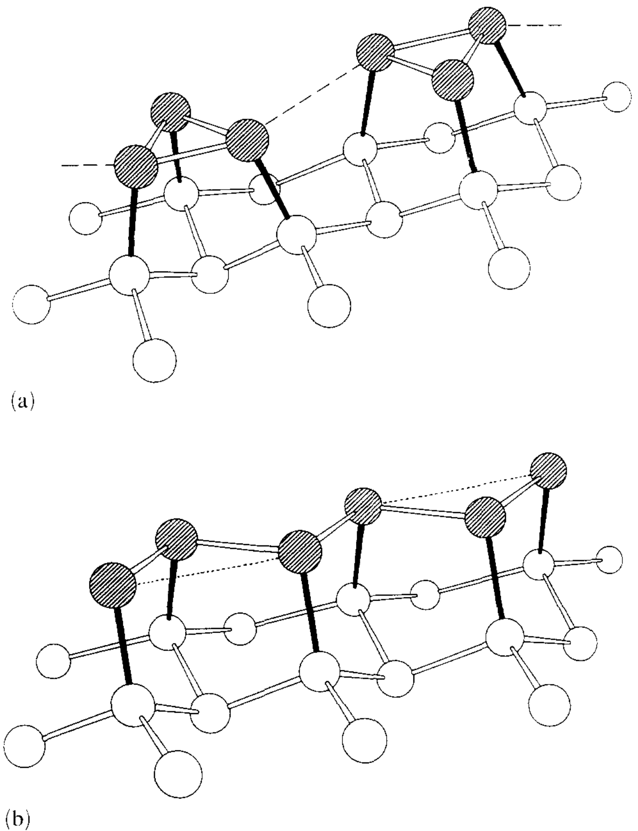

Fig. 4. Illustration of a possible pathway leading from the trimer geometry (a) to the chain geometry (b) by bond exchange. New bonds are formed where indicated by dashed lines in (a), and eliminated bonds are shown by dotted lines in (b).

transformation from trimers to chains: one switch per triplet of group V atoms, or one third of a bond exchange per group V atom is required. In contrast, going from either of these geometries to the substitutional geometry requires a large change in connectivity, and the elimination of all group-V–group-V bonds in favor of formation of group-V–substrate bonds. Thus, at least three bonds per group V atom have to be reformed, a process which is likely to be energetically more costly than the trimer-to-chain transformation described above. Although it is difficult to calculate all the relevant energies for such processes, these arguments suggest that transforming from trimers to chains is kinetically allowed, whereas transforming from either of those structures which involve self-bonded adsorbate units to the substituional structure is disallowed.

4. Simulation of growth in the presence of surfactants

The most interesting aspects of surfactant mediated growth concerns first the mechanisms by which the

adsorbates segregate during growth, and second how their presence affects the growth process. Both issues are very difficult to address from first-principles calculations, since there is essentially an unlimited set of possibilities that may play an important role. To address the first issue we offer again qualitative arguments based on structural features of the different atomic arrangements. As for the second issue, we study through Monte Carlo simulations a heuristic model that captures some of the features of surfactant mediated growth.

The segregation of the adsorbates to the surface must be a process that is not kinetically hindered by large energy barriers. In the case of growth of Ge on Si(111), there are probably several possible pathways by which the group V atoms can segregate to the surface by exchanging positions with newly deposited Ge atoms. By considering the bonding topology of the different geometries on Si(111), it appears that atoms in self-bonded adsorbate units would segregate more easily, since each adsorbate atom has only one covalent bond to the substrate. The remaining two covalent bonds to other adsorbate atoms need never break during the segregation. In contrast, atoms in the substitutional geometry would find it very difficult to segregate to the surface, since all three of their covalent bonds to the substrate need to be severed during segregation. These considerations indicate that Sb, which naturally prefers the trimer or chain geometries (see Fig. 3), is a better choice for surfactant than either P or As which prefer the substitutional geometry. A recent experimental work that compared the effectiveness of these elements in enhancing layered growth during Si homoepitaxy on Si(111) found precisely the effect predicted by the above analysis [19]. Specifically, Sb proved much more effective in promoting layered growth than As.

An even more difficult question is how exactly is growth affected when a surfactant is present. To obtain some insight into this problem we consider and simulate the behavior of a simple solid-on-solid model. The features of this model are derived from the preceding discussion of energetic and structural aspects of surfactant monolayers. We first describe the model in detail.

(1) The surfactant always covers the entire top layer on which newly deposited atoms arrive. This is necessary for passivation of the surface and implies efficient segregation of the surfactant atoms.

(1) Owing to passivation of the surface by the surfactant, the newly deposited atoms interact weakly with the top-most adsorbate layer and can therefore move freely on the surface, i.e. the activation energy for surface diffusion is small.

(3) There exist pathways by which the newly deposited atoms exchange position with surfactant atoms (or units of atoms) and thereby become embedded below the adsorbates. We denote the activation energy for such processes as ε_a. This activation energy is unknown, and is considered a free parameter in the simulations.

(4) The atoms that have been embedded below the adsorbate layer diffuse very slowly, because bulk diffusion has an activation energy much larger than surface diffusion and larger than ε_a.

(5) If the newly deposited atoms arrive at a step on the surfactant-covered surface, they exchange positions with the surfactant atoms in their neighborhood and become embedded below them, with an activation energy smaller than ε_a. This is justified by the observation that in the neighborhood of steps there are usually unsatisfied dangling bonds, which lead to higher reactivity. It is natural to expect that step geometries will be easier to perturb toward achieving local equilibrium, which involves placing the surfactant atoms on top.

The relative energies implied by this model are shown schematically in Fig. 5. This relative energy landscape allows for considerable simplification of the simulation, based on the following two assumptions.

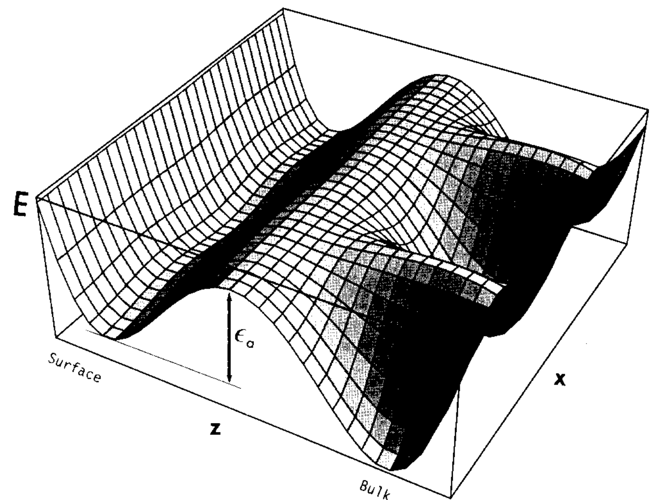

Fig. 5. Schematic representation of the different energy terms affecting the kinetics during surfactant mediated growth. The z coordinate denotes the position of newly deposited atoms along the growth direction. The region labeled "Surface" corresponds to the newly deposited atoms being on top of the adsorbate layer, while the region labeled "Bulk" corresponds to the deposited atoms being embedded under the adsorbate layer. The x coordinate is along the surface plane (perpendicular to the growth direction). Motion along this coordinate is characterized by small activation energy (leading to very fast diffusion) when the newly deposited atoms are on the surface, and very large activation energy (leading to very slow diffusion) when the atoms are in the bulk. The activation energy for exchange between newly deposited atoms and adsorbate atoms on a terrace ε_a is indicated.

(a) For processes that have activation energies smaller than ε_a (such as surface diffusion), we assume that they take place without any hindrance. (b) For processes that have activation energies larger than ε_a (such as bulk exchange), we assume that they never occur during the simulation. Neither of these two assumptions introduces any additional constraints on the system. They merely set the shortest and longest time scales in the simulation. Specifically, the shortest time scale τ_S is given by

$$1/\tau_S = \nu_S \exp[-\varepsilon_S/k_B T] \quad (1)$$

where ε_S is the highest activation energy that is lower than ε_a and ν_S is the corresponding attempt frequency. Similarly, the longest time scale τ_L is given by

$$1/\tau_L = \nu_L \exp[-\varepsilon_L/k_B T] \quad (2)$$

where ε_L is the lowest activation energy that is higher than ε_a and ν_L is the corresponding attempt frequency. We take all attempt frequencies, including that of exchange between newly deposited atoms and surfactants on a terrace, to be of the same order of magnitude. As long as ε_S and ε_L differ from ε_a by more than a few $k_B T$, assumptions (a) and (b) are reasonable. In Si, the calculated activation energies for surface diffusion are of order $\varepsilon_S \approx 0.5$ eV [20], and for bulk exchange of order $\varepsilon_L \approx 4$ eV [21]. The value of ε_a is expected to lie between these limits, since it corresponds to processes that involve a greater disturbance than surface diffusion (so that $\varepsilon_a > \varepsilon_S$) and a smaller disturbance than exchange of atoms in the bulk, where they are more constrained (so that $\varepsilon_a < \varepsilon_L$). Thus, there is a range of about 3 eV for the value of ε_a in which all the necessary conditions are satisfied. Within the model described above, the surface diffusion is free (the newly deposited atoms move randomly and freely on top of the surfactant layer), the bulk diffusion is non-existent (the newly deposited atoms are frozen once they have been embedded below the surfactant), and exchanges between newly deposited atoms and surfactant atoms take place with a probability equal to $\exp[-\varepsilon_a/k_B T]$ on top of flat regions, and equal to unity at steps.

We considered two types of model, one in which both the surface diffusion and the probability of attachment at steps are isotropic, and a second in which diffusion and attachment are anisotropic. The second model was inspired by the structure of the Si(100) substrate, which is highly anisotropic in the two directions along dimer rows and perpendicular to them. This structure is known to produce a large anisotropy in the diffusion and the shape of islands grown on Si(100). For example, diffusion along the rows is several orders of magnitude faster than diffusion perpendicular to them [22]. Similar anisotropy should exist in the sticking probability of atoms on different sides of islands, which accounts for their anisotropic shape. We have asumed that both the diffusion and the sticking probability are anisotropic by a factor of 10^2 in the two inequivalent directions. The direction of anisotropy changes by 90° for each added layer, consistent with the 90° rotation of the dimer row direction on the Si(100) surface on addition of a monolayer.

Finally, we assume that the deposition rate is sufficiently slow so that the newly deposited atoms do not have the opportunity to agglomerate before they can exchange positions with surfactant atoms somewhere on the surface. This feature is motivated simply by computational considerations. It allows for much faster simulations, which enabled us to study the deposition of a large amount of material onto a large substrate, thus elimianting spurious effects due to finite size. This completes the description of the model.

We have performed extensive MC simulations with this model, on square lattice substrates of sizes ranging from 100×100 sites to 1000×1000 sites, with periodic boundary conditions (the largest lattice would correspond to an Si(100) substrate of size approximately 4000×4000 Å^2). We studied a range of values of the free parameter $k_B T/\varepsilon_a$. The different values of the free parameter can be thought of as corresponding to different types of surfactant at fixed growth temperature, or to the same surfactant (fixed ε_a) at various temperatures.

The simulations reveal that there are two clearly distinguishable modes of growth, depending on the value of the free parameter. For low enough values of $k_B T/\varepsilon_a$ (less than 0.1) smooth layer-by-layer growth is obtained. This is directly evident from the roughness, measured by the deviation of the local height $h(\boldsymbol{x},t)$ from the average height $\bar{h}(t)$ as a function of time t (the time is proportional to the number of deposited layers, assuming a constant rate of deposition). This deviation is defined by

$$w^2(t) = \langle [h(\boldsymbol{x}, t) - \bar{h}(t)]^2 \rangle \quad (3)$$

where $\langle\ \rangle$ denotes an average taken over the two-dimensional lattice. The behavior of $w^2(t)$ is shown in Fig. 6 for $k_B T/\varepsilon_a = 0.05$. In the isotropic model it exhibits periodic oscillations, with the minima corresponding to complete layers and the maxima corresponding to half-layer intervals. The maximum value of $w^2(t)$ is 0.25, exactly what is expected for half a layer deposited on top of a flat surface. The oscillations persist for as long as we have run the simulation, without any perceptible changes. For the anisotropic model, there are no clear oscillations since the anisotropy introduces a certain amount of roughness by itself. The average value, however, remains constant and does not increase in the course of the simulation, for as long the simulation runs (up to 3000 layers for

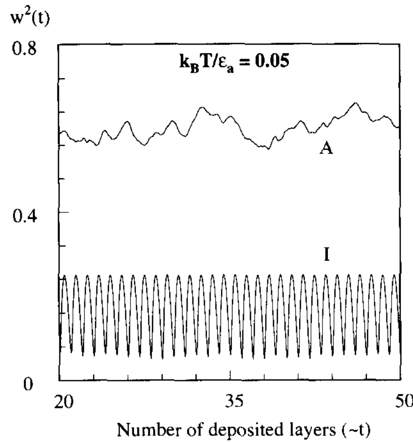

Fig. 6. Roughness $w^2(t)$ as a function of number of deposited layers (proportional to t) for $k_BT/\varepsilon_a = 0.05$, for the isotropic (I) and anisotropic (A) models. A short time interval (corresponding to deposition of 30 layers between the 20th and 50th layers) is shown to make the oscillations visible. This behavior is unchanged for as long as the simulation was continued (up to 500 layers). The minima of oscillations in the isotropic model correspond to completion of full layers.

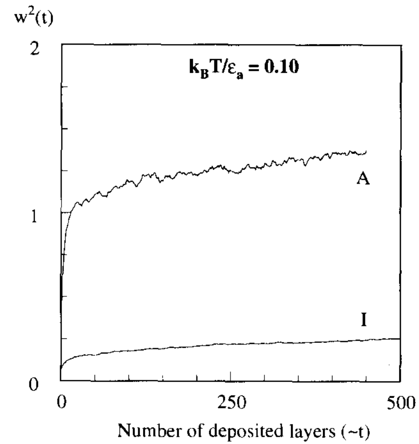

Fig. 7. Same as in Fig. 6 for $k_BT/\varepsilon_a = 0.10$. For the isotropic model values of w^2 at full monolayer intervals are shown (corresponding to the minima of oscillations in Fig. 6). The steadily increasing w^2 in both the isotropic and anisotropic models signifies a rough surface.

the 100 × 100 lattices and to 500 layers for the 1000 × 1000 lattices).

When $k_BT/\varepsilon_a \geq 0.1$, qualitatively different behavior is obtained. This is shown in Fig. 7, where $w^2(t)$ is plotted for deposition up to 500 layers. For both the isotropic and the anisotropic models, $w^2(t)$ increases monotonically with time. This behavior is qualitatively unchanged at higher values of k_BT/ε_a. The rate of increase of $w^2(t)$ becomes larger for larger values of k_BT/ε_{aq}. An increasing $w^2(t)$ signifies a rough surface.

For a more detailed understanding of the system during growth, we show in Fig. 8(a) a top view of the anisotropic model for the 1000 × 1000 lattice after 50 layers of deposition, for $k_BT/\varepsilon_a = 0.05$. The different colors indicate different depth levels. While there are five clearly distinguishable layers, the surface is overall rather flat. In Fig. 8(b) a perspective close-up view of the central 200 × 200 region of this lattice is shown which demonstrates the flatness of this system. This image would correspond to a region of Si(100) equal to about 800 × 800 Å^2, while each vertical step would be 1.36 Å. Figs. 9(a) and 9(b) are the corresponding images for the case $k_BT/\varepsilon_a = 0.10$. The qualitative difference in the growth mode is evident, both in the top view and in the perspective close-up view. For this value of k_BT/ε_a the overlayers have a considerable degree of roughness, which increases with time. The behavior of $w^2(t)$, while suggestive of the qualitative difference in growth mode, does not contain enough information about the structure of the overlayers. Specifically, the value of $w^2(t)$ is only slightly higher than unity in the anisotropic model at $k_BT/\varepsilon_a = 0.10$, for deposition up to 500 layers (see Fig. 7). This indicates a relatively small variation in height. Indeed, Fig. 9 reveals that there are seven different layers, just two more than in Fig. 8. The quality of the film in Fig. 9, however, is evidently much worse than that of Fig. 8. Other quantities such as height-height correlations, also display the qualitative difference in growth mode depending on the value of k_BT/ε_a, albeit somewhat less directly than the film images presented in Figs. 8 and 9.

5. Discussion and conclusions

The first-principles calculations and growth simulations described above lead to the following conclusions.

(1) On surfaces of semiconductors which are passified by full monolayer coverage of adsorbates, the elements that can easily segregate to the surface are those that form self-bonded adsorbate units. Adsorbates that prefer geometries not involving such units will prove more difficult to segregate. On the Si(111) substrate for example, As and P prefer the latter type of geometry, while Sb prefers structures that comprise self-bonded adsorbate units such as trimers or chains. To the extent that segregatin of the adsorbates is a necessary condition for altering the mode of growth, the adsorbates that form self-bonded adsorbate units are the most likely candidates for good surfactants.

(2) An important quantity that can affect the mode of growth is the activation energy ε_a for exchange

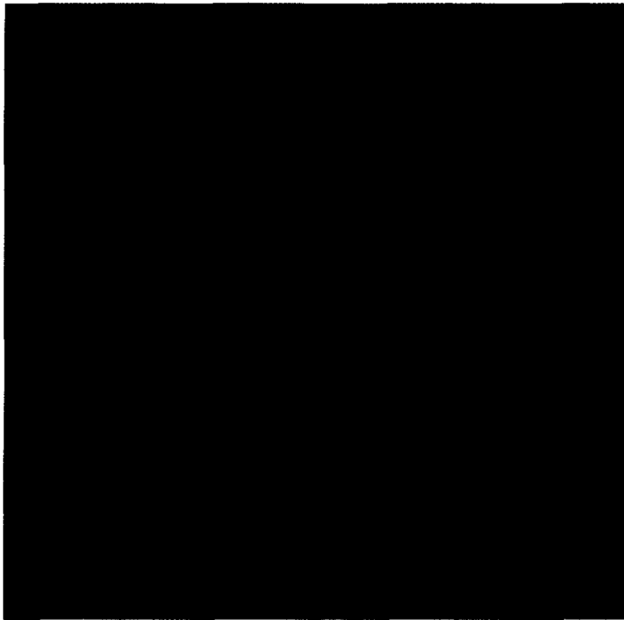

(a)

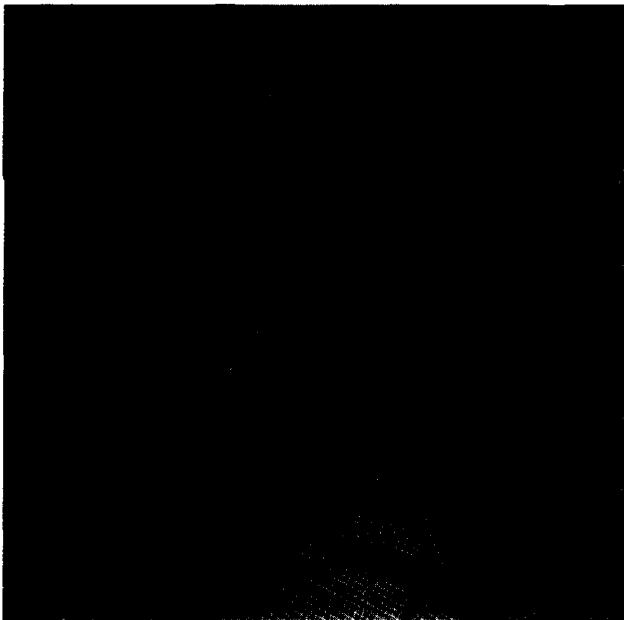

(b)

Fig. 8. (a) Top view of 1000×1000 lattice after deposition of 50 layers in the anisotropic model, for $k_B T/\varepsilon_a = 0.05$. The general features remain unchanged at higher deposition. The color code indicates different heights, from blue (lowest level) to red (highest level). Five different heights are present. (b) Perspective close-up view of the central 200×200 region, in which the island features are apparent.

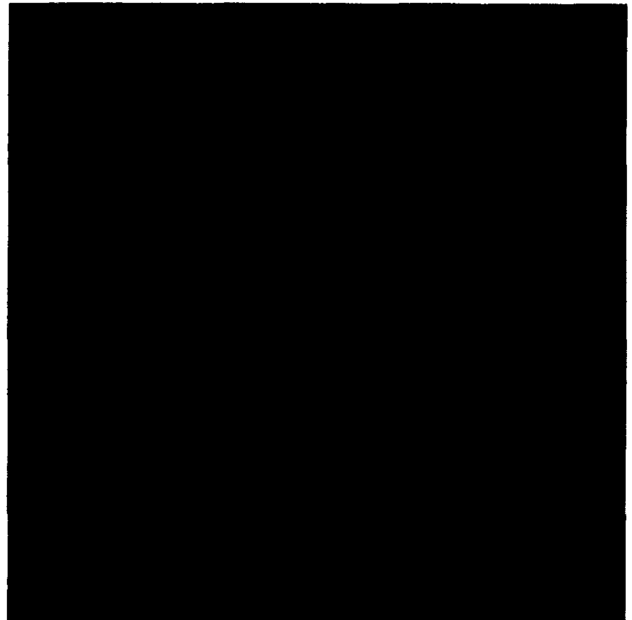

(a)

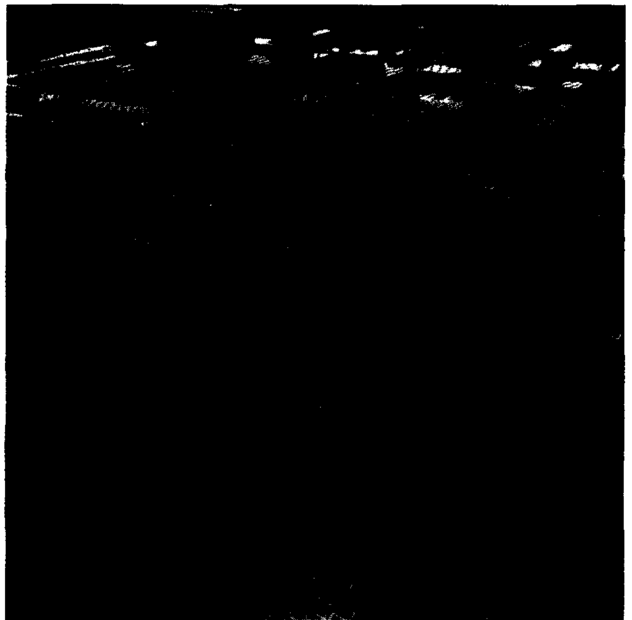

(b)

Fig. 9. Same as in Fig. 8, for $k_B T/\varepsilon_a = 0.10$. Seven different heights are present. The film roughness is much more pronounced.

between the newly deposited atoms and the surfactant atoms. For deposition rates that are slow enough to avoid agglomeration of the newly deposited atoms on top of the adsorbate layer, the value of $k_B T/\varepsilon_a$ determines the type of growth. For small values of $k_B T/\varepsilon_a$ smooth films are obtained, while for higher values there exists considerable roughness. The critical value of $k_B T/\varepsilon_a$ that separates the two types of growth appears to be around 0.1. Thus, in the presence of a surfactant characterized by ε_a, smooth films can be grown for temperatures lower than $0.1\varepsilon_a$. This is different than the normal case of growth, where the temperature typically has to be high enough to enhance

diffusion and avoid nucleation of islands, leading to smooth growth. Surfactants can suppress island nucleation at terraces by allowing newly deposited atoms to diffuse fast to the nearest step where they become embedded under the adsorbate atoms. The fast diffusion on top of the surfactant is due to the passive nature of the adsorbate layer, which makes it difficult for the newly deposited atoms to interact strongly with the adsorbates on the terraces. If the temperature exceeds $0.1\varepsilon_a$, island nucleation at terraces becomes important, leading to rough growth.

Both conclusions rest on the assumption that a full monolayer of adsorbates is needed to produce the desired changes in growth mode. This appears to be the case for semiconductor surfaces, which are typically rendered more stable and passive by monolayers of adsorbates such as group V elements. In systems where partial coverage can drastically affect the growth kinetics, a different analysis must be carried out. Examples of such systems are metal surfaces, on which a small fraction of a monolayer coverage can have a dramatic impact by changing the structure and the kinetics of steps [23].

Acknowledgment

This work was supported by the Office of Naval Research, Contract N00014-92-J-1138. The calculations were carried out at the Cornell National Supercomputer Facility.

Appendix A

The first-principles calculations reported here are based on density functional theory in the local density approximation [24,25]. The ions are represented by norm-conserving non-local pseudopotentials from Bachelet et al. [26], which make it possible to avoid treating the core electrons explicitly. This approach can provide reliable total-energy comparisons for a variety of physical systems, including metals, insulators and semiconductors, as has been shown by extensive applications over the past two decades (for a recent review see Ref. [27]). Here, we use the exchange-correlation functional proposed by Perdew and Zunger [28], and a plane wave basis for expanding the electronic wavefunctions. Plane waves with kinetic energy up to 10 Ry are included in the basis. Since the different structures we compared have different periodicities and unit cells, the sampling of reciprocal space has to be done in a careful manner. We found that a Monkhorst–Pack [29] set of 16 points in the surface Brillouin zone is needed for the structures with largest periodicity ($\sqrt{3}\times\sqrt{3}$), with correspondingly larger sets for the structures with smaller periodicity, (2×1) and (1×1). The surfaces are modeled by slabs which are periodically repeated in the direction perpendicular to the surface. The slabs consist of 12 atomic layers separated by vacuum regions equivalent to three bond lengths of bulk Si. Inversion symmetry is used to facilitate the computations and to eliminate charge transfer between the two sides of the slab. Full relaxation of the atomic geometries is included by minimizing the magnitude of forces on the ions, calculated through the Hellmann–Feynman theorem. In the relaxed equilibrium configurations the forces are smaller than 5 mRy au^{-1}. With these computational parameters, we find that relative energy differences are converged to about 10 meV per adatom. This allows for meaningful comparisons of the relative energies as shown in Fig. 3.

References

[1] A. Madhukar, *Thin Solid Films, 231* (1993) 8.
[2] T. Pearsal (ed.), *Strained Layer Epitaxy*, Vols. 1 and 2, Academic Press, New York, 1990.
[3] M. Copel, M.C. Reuter, E. Kaxiras and R.M. Tromp, *Phys. Rev. Lett., 63* (1989) 632.
M. Copel, M.C. Reuter, M. Horn von Hoegen and R.M. Tromp, *Phys. Rev. B, 42* (1990) 11682.
[4] M. Horn-von Hoegen, F.K. LeGoues, M. Copel, M.C. Reuter and R.M. Tromp, *Phys. Rev. Lett., 67* (1991) 1130.
[5] J. Falta, M. Copel, F.K. LeGoues and R.M. Tromp, *Appl. Phys. Lett., 62* (1993) 2962.
[6] D.J. Eaglesham, F.C. Unterwald and D.C. Jacobson, *Phys. Rev. Lett., 70* (1993) 966.
[7] R.M. Tromp and M.C. Reuter, *Phys. Rev. Lett., 68* (1992) 954.
[8] B.D. Yu and A. Oshiyama, *Phys. Rev. Lett., 71* (1993) 585.
[9] Z. Zhang and M.G. Lagally, *Phys. Rev. Lett., 72* (1994) 693.
[10] A.-L. Barabasi, *Phys. Rev. Lett., 70* (1993) 4012.
[11] E. Kaxiras, *Europhys. Lett., 21* (1993) 685.
[12] F. Boszo and Ph. Avouris, *Phys. Rev. B, 43* (1991) 1847.
[13] R.S. Becker, B.S. Swartzentruber, J.S. Vickers, M.S. Hybertsen and S.G. Louie, *Phys. Rev. Lett., 60* (1988) 116.
[14] P. Martensson, G. Meyer, N.M. Amer, E. Kaxiras and K.C. Pandey, *Phys. Rekv. B, 42* (1990) 7230.
[15] L. Pauling, *The Nature of the Chemical Bond and the Structure of Molecules and Crystals*, Cornell University Press, Ithaca, NY, 1960.
[16] K.C. Pandey, *Phys. Rev. Lett., 47* (1981) 223.
[17] J.E. Northrup and M.L. Cohen, *Phys. Rev. Lett., 49* (1982) 1349.
[18] Y.M. Huang, J.C.H. Spence, O.F. Sankey and G.B. Adams, *Surf. Sci., 256* (1991) 344.
[19] M. Horn-von Hoegen, J. Falta, M. Copel and R.M. Tromp, preprint.
[20] G. Brocks, P.J. Kelly and R. Car, *Phys. Rev. Lett., 66* (1991) 1729.
[21] K.C. Pandey, *Phys. Rev. Lett., 57* (1986) 2287.
[22] Y.W. Mo, J. Kleiner, M.B. Webb and M.G. Lagally, *Phys. Rev. Lett., 67* (1991) 1998.

[23] G. Rosenfeld, R. Servaty, C. Teichert, B. Poelsema and G. Comsa, *Phys. Rev. Lett., 71* (1993) 895.
[24] P. Hohenberg and W. Kohn, *Phys. Rev., 136* (1964) B864.
[25] W. Kohn and C.J. Sham, *Phys. Rev., 140* (1965) A1133.
[26] G.B. Bachelet, D.R. Hamann and M. Schlüter, *Phys. Rev. B, 26* (1982) 4199.
[27] W.E. Pickett, *Comput. Phys. Rep., 9* (1989) 117.
[28] J. Perdew and A. Zunger, *Phys. Rev. B, 23* (1984) 5048.
[29] H.J. Monkhorst and J.D. Pack, *Phys. Rev. B, 13* (1976) 5188.